Nuclear Data for Science and Technology (1988 MITO), 165- 168, Copyright © 1988 JAERI.

THE MEASUREMENT OF ACCURATE TOTAL CROSS-SECTIONS FOR LEAD AND CARBON IN THE ENERGY RANGE 50 eV TO 100 keV

J. Schmiedmayer
Institute of Nuclear Physics, Technical University, Vienna, Austria

M. C. Moxon
Harwell Laboratory, Didcot, Oxon. UK

The transmission of Pb and C has been accurately measured in the neutron energy range 50 eV to 100 keV using a 150 m flight path on the fast neutron target cell of HELIOS. The measurements were made with a ^{10}B loaded liquid scintillator using a new fast electronics system capable of recording simultaneously, with a dead time of 10 ns, both time-of-flight and pulse amplitude. The neutron time-of-flight resolution and backgrounds in the experiment were determined from measurements on W, Co, Mn, and ^{238}U by using the REFIT resonance analysis code. The ^{10}B loaded scintillator gave better signal to background ratios than other normally used systems and recording both time-of-flight and pulse height information enabled accurate cross-section values to be obtained from the data. The zero energy free atom scattering cross-sections for Pb and C are determined to be 11.258±0.005 and 4.7438±0.0020 barns respectively. After correcting for neutron-electron, Schwinger and resonance scattering effects the electric polarizability of the neutron (α_n) is determined from the energy dependence of the Pb total cross-section to be $(1.2\pm1.0)\times10^{-3}$ fm^3. The experimental measurements and the analysis of the results are discussed.

Keywords: time-of-flight system, detectors, Pb, C, total cross-section, resonance parameters, 50 eV - 100 keV, electric polarisability of the neutron

1. Introduction

The precise value of the total cross-section of lead and carbon in the energy range < 50 keV neutron energy is of special scientific and technological interrest. Carbon is an important element in nuclear technology and lead is the only heavy element with only a few small resonances. Their contributions to the total cross-section are small and calulable. From the accurate energy dependence of the Pb cross-section some of the fundamental electric properties of the neutron, like neutron-electron scattering and the electric polarizability of the neutron, can be extracted [1]. Carbon, for its low Z, serves thereby as a null test of the measurement.

To achieve the desired accuracy of $\Delta\sigma/\sigma \leq 10^{-3}$ substantial improvements to measurement techniques had to be made. Data has to be recorded at very high speeds. Backgrounds, detector variations, bias shifts and other unforseeable irregularities in the measurement system have to be easily recognized. This can be achieved by knowing the pulse height or pulse shape distribution of the detection system for each time-of-flight (TOF) channel. A fast multi-parameter TOF system with 10 ns dead time, based on a new analogue-time-digitizer, as used in high energy physics experiments [2,3], capable of simultaneous time and analogue measurement was developed [1,4]. The signal to background ratio was significantly improved by the use of a ^{10}B-loaded liquid scintillator [1,5] as a neutron detector, which has a very high detection efficiency for keV neutrons and low γ-ray sensitivity. The experimental setup, measurements and the analysis of the results are discussed.

2. Measurement system:

Analog time digitizer

The centerpiece of the CAMAC module, designed for time-of-flight and high energy physics applications, is a 8 bit 100 MHZ flash ADC SDA 8010 from Siemens and a time digitizer with a maximum time resolution of 20 ns and a total time range of 4.9 ms. The whole digitizing process (8 bit analog and 16 bit time information) including the storage in an internal buffer is done with a deadtime of 10 ns [4].

A linear response curve was chosen for the FADC to measure equally positive and negative signals, and a DC bias level, controlled by an external 20 turn potentiometer, allows optimal adjustment of the input signal.

The time digitizer was basically designed to be used in neutron TOF experiments up to a few keV neutron energy. The whole time range is divided into 4 regions each 16384 (14 bit) channels long. The minimum time resolution (1st time region) is 20 ns (2 times the basic clock frequency) as defined by the 50 ns FWHM moderation time jitter for 1 keV neutrons [6]. There is a 2 fold increase in the channel width for each subsequent region (see Tab.1).

Table 1: Characteristics of the time scaler.

timeregion		channel width	length
1	16384 chan. (14 bit)	20 ns	0.32768 ms
2	16384 chan. (14 bit)	40 ns	0.65536 ms
3	16384 chan. (14 bit)	80 ns	1.31072 ms
4	16384 chan. (14 bit)	160 ns	2.62144 ms
total	65536 chan. (16 bit)		4.91520 ms

The time resolution can easyly be improved to 10 ns by using the 100 MHZ clock as a time basis for the first time region. With time interpolation techniques as described in [3] time resolutions of 2.5 ns and better can be obtained at the same data taking speed and deadtime.

Data Aquisition System

The present data aquisition system is based on a PDP 11/73 computer with 4 MB memory. It can take data from up to 4 independent FADC modules, 20 scalers and various auxiliary data (eg. electron pulse shape of the linac, counts per burst for each detector). Up to 9 sample positions are allowed.

The data from each FADC module is transfered, after each machine cycle, into a software buffer in the computer and, during the next cycle, filled into the TOF-analogue histograms. With the use of lookup tables a variety of different analog and time resolutions can be incorporated in one histogram at a very high datataking speed (in a test up to 40000 datawords were read and processed per second)

A typical TOF pulse height histogram measured at the 150 m flight path with a Mn filter in the beam is shown in Fig.1. The dips in the TOF spectrum correspond to the 0.336, 1.1, 2.4, 7.1, 8.8 keV resonances used for background measurement. In the pulse height spectrum of the ^{10}B liquid scintillator, the crunch boundary between the 2 analog regions is shown. The time dependence of the background can be determined from the data in the the overflow and in the low pulse height channels.

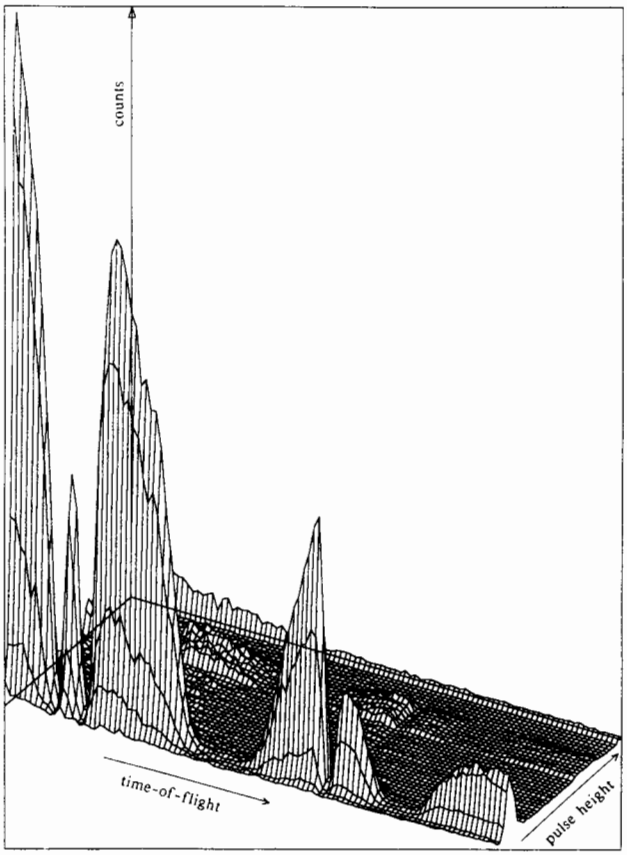

Fig. 1: Pulse height - TOF spectrum for a Mn filter measured at the 150 m flightpath in a transmission experiment at the HELIOS neutron source at HARWELL.

The ^{10}B-loaded liquid scintillator

Due to their high hydrogen (65%) and ^{10}B (5%) content ^{10}B-loaded liquid scintillators (like BC523-A or NE311-A) offer many advantages over other neutron detectors. They have compact size, and a high detection efficiency for neutrons up to 100 keV energies via the $^{10}B(n,\alpha)^{7}Li$ reaction. Faster neutrons are detected by recoil protons. Good pulse-shape discrimination properties have been reported for various scintillator solutions [7].

A neutron entering the scintillator undergoes elastic scattering (mainly on hydrogen), until it is captured by in a $^{10}B(n,\alpha)^{7}Li$ reaction which has two branches [8].

$$^{10}B + n \begin{cases} \nearrow\ ^{7}Li + \alpha + 2.790\ \text{MeV} & (6.3\%) \\ \searrow\ ^{7}Li^{*} + \alpha + 2.312\ \text{MeV} & (93.7\%) \\ \qquad \searrow\ ^{7}Li + \gamma\ (478\ \text{keV}) \end{cases} \qquad (1)$$

The light output is primarily due to the α-particle and is equivalent to that of a 60 keV electron. The 478 keV γ-ray emitted in 93.7% of the $^{10}B(n,\alpha)$ reactions has a small probability of beeing detected in the scintillator.

The detection response of ^{10}B-loaded liquid scintillators in various detector geometries and for neutrons below 50 keV has been calculated using a simple Monte-Carlo code [1,5].

The advantage of the ^{10}B-loaded detector, especially in the energy range above 100 eV (Tab.2) is best seen by comparing the ratios between the detection efficiencies for neutrons and the γ-rays (ε_n, ε_γ). For 100 eV neutrons the ^{10}B-loaded liquid scintillator is superior to a ^{6}Li-glass scintillator by a factor 4. At 10 keV he is more then a factor 10 better [1].

Table 2: Comparison of the detection efficiency for neutrons and 2.2 MeV γ-rays in a ^{10}B-loaded liquid scintillator and a ^{6}Li-glass detector.

scintillator	thick-ness	$\varepsilon_{2.2MeV}$	ε_n 1 eV	100 eV	10 keV
^{6}Li-glass	1 cm	0.10	.84	.19	.021
^{10}B-liquid	1 cm	0.036	.88	.34	.09
	2 cm	0.072	.98	.66	.28

A pulse height spectrum of a ^{10}B liquid scintillator for 5 keV neutrons measured on the 150 m flightpath is shown in Fig.2. The α peak of the $^{10}B(n,\alpha)$ reaction and the Compton edge from the few 478 keV γ-rays converting in the scintillator are clearly seen. Superimposed is a pulse height spectrum for the background as measured with a thick polyethene filter in the beam. The channels above and below the neutron pulse height can be used for background determination in each TOF channel. The signal to background ratio at the α peak is about 300 : 1.

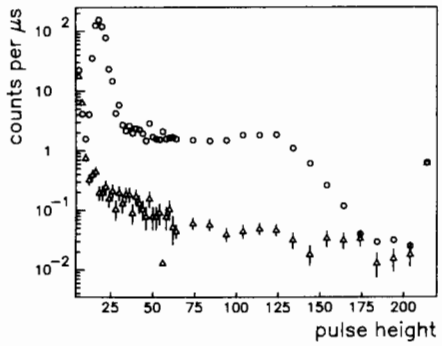

Fig. 2: Pulse height for 5 keV neutrons (o) and background (Δ) detected in a 2 cm thick ^{10}B-loaded liquid scintillator (BC523-A) measured with the analog time digitizer.

The background measurements with W, Mn, Co, filters and ^{238}U data was used for the determination of the time resolution parameters of the 20 mm thick ^{10}B-loaded liquid scintillator using the REFIT [9] resonance analysis computer code. The decay parameters and the mean capture times (Fig.3) derived from REFIT are in good agreement whith the values from the Monte-Carlo calculations [1,5].

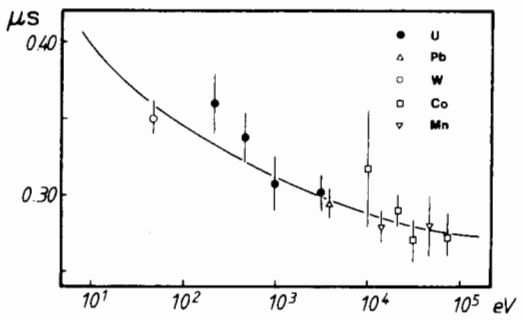

Fig. 3: Mean capture time for a neutrons in a 2 cm thick ^{10}B-loaded liquid scintillator (BC523A) as evaluated by the REFIT calculations. The results are in good agreement with the Mont-Carlo calculations (——).

3. Measurement:

The neutron transmission of lead and carbon were measured at the 150 m flight path at the Fast Neutron Target of the HELIOS neutron source at HARWELL using the new TOF setup described above. The neutrons were detected with a 20 mm thick ^{10}B-loaded liquid scintillator (BC523A from *Bicron*) mounted directly on a Hamamatsu R1250 phototube, selected for good photocathode efficiency and low afterpulsing [10]. The PM was gated by a setup

described in [11] to reduce the effects from the gamma flash.

Data were taken in 3 periods of 6 days each with the HELIOS electron linac running on 150 Hz and 50 ns pulse width. Overlap neutrons were reduced to an insignificant level by the use of a boron poisoned moderator and a ^{10}B filter. Lead and carbon samples of about equal transmission were measured together with resonance filters (W, Mn, Co, Al) and a polythene absorber for background determination. Thick samples of transmissions in the range from 50% down to 4% were used for optimal determination of the flat cross-sections, and as a good test for systematic errors.

4. Data evaluation

The 2-dimensional TOF - pulse height histograms were first inspected for bias shifts, detector variations and other irregularities. Some of the data had to be rejected. Afterwards the data was summed in selected pulse height regions corresponding to neutron and background data. This selected data was the used in the further data evaluation.

Background

The background (typical < 1%) was evaluated using the black resonances of

W 7.6 eV, 20 eV, 184 eV,
Mn 336 eV, 1.1 keV, 2.4 keV, 7.1 keV, 8.8 keV,
Co 132 eV, 4.3 keV, 5.0 keV,
Al 34 keV, 87 keV,
a polythene absorber < 100 keV

and the measured detector pulse height distribution. All the background data were fitted to an exponential decaying time dependence (Fig.4). γ-ray attenuation coefficients were included for all samples and filters.

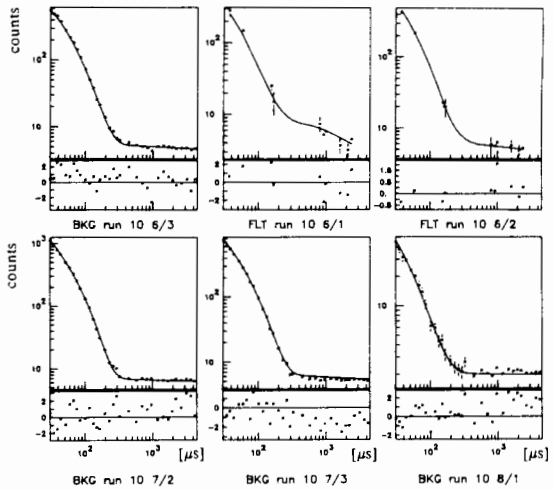

Fig. 4: Backgrond data for different samples from black resonances (FLT) and selected pulse height channels (BKG). The solid line shows a fit using a simple model including γ-ray attenuation cross-sections for the samples and filters.

Total Cross-Section

After background subtraction the transmissions were calculated and an energy dependent vacuum correction applied. To illustrate the quality of the data the averaged transmissions in the energy range from 50 eV to 300 eV are plotted versus sample thickness (Fig.5). Even very thick samples with only a few percent transmission show no systematic deviations. The free atom total cross-section in that energy range is evaluated for lead to σ_s = 11.258 (5) b and for carbon to σ_s = 4.7438 (20) b. The values are in perfect agreement with the best measured values of the total cross-section at zero neutron energy (lead: 11.258(4) b [12] and carbon: 4.746(2) b [13]).

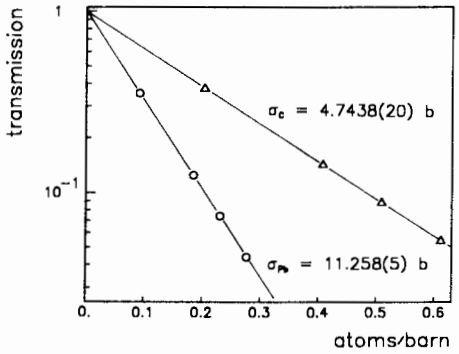

Fig. 5: Averaged transmission of lead and carbon plotted versus sample thickness.

Carbon

An optimal fit of an effective range approximation to the measured total scattering cross-section in the energy range 50 eV < E < 100 keV gives:

$$\sigma_C(E) = 4.7435(16) - 3.41(24)\times E \qquad E \text{ in [MeV]} \quad (2)$$

This result can be compared to parametrisations obtained in a much wider energy range up to several MeV. Heaton et al. get in the energy range 1 keV < E < 15 MeV [14]

$$\sigma_C(E) = 4.757 - 3.419\times E + 1.548\times E^2 - 0.328\times E^3 \quad (3)$$

and Lachkar gets for 10 eV < E < 2 MeV [15]

$$\sigma_C(E) = 4.725 - 3.251\times E + 1.316\times E^2 - 0.227\times E^3 \quad (4)$$

Lead

The whole data set for lead was analyzed with REFIT (Fig.6) and new highly accurate parameters (Γ_n) were extracted for some of the bigger resonances. With the new parameter set (Tab.3), the absorption and scattering cross-section of each isotope was correctly reproduced using the same potential scattering radius for all isotopes (R_0=9.73 fm). For the thermal incoherent scattering cross-section we obtain 3.3 mb, which is in good agreement with the measured value of 3.0(7) mb [16].

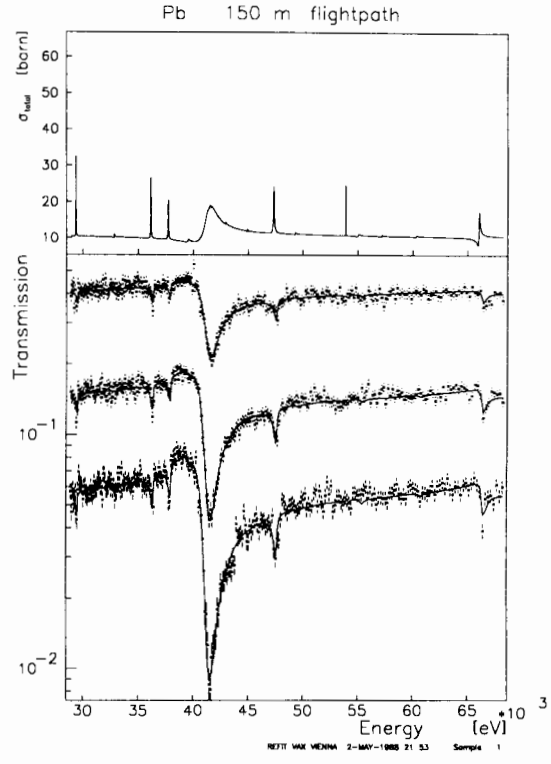

Fig. 6: REFIT calculation for 3 different Pb samples.

Table 3: Extracted resonance parameters for Pb. Isotope, spins and radiation widths (Γ_γ) used in the analysis are from ref. [13].

Nuclid	L	J	Energy [eV]		Γ_n [eV]	
^{204}Pb	0	1/2	1688.	(2)	3.32	(10)
^{204}Pb	0	1/2	2481.	(3)	5.45	(20)
^{207}Pb	1	2	3063.6	(9)	0.13	(3)
^{206}Pb	1	3/2	3357.1	(5)	0.24	(5)
^{204}Pb	0	1/2	6699.	(4)	4.8	(11)
^{204}Pb	0	1/2	8354.	(3)	40.2	(25)
^{204}Pb	0	1/2	12916.	(7)	52.2	(55)
^{207}Pb	1	1	16768.	(4)	36.3	(13)
^{206}Pb	1	1/2	25411.	(6)	53.2	(22)
^{207}Pb	1	2	29372.	(14)	18.	(2)
^{206}Pb	1	1/2	36217.	(11)	37.3	(32)
^{207}Pb	1	1	37704.	(18)	47.7	(46)
^{207}Pb	0	1	41238.	(9)	1121.	(13)
^{206}Pb	1	1/2	47421.	(19)	98.9	(64)
^{206}Pb	0	1/2	65954.	(36)	93.	(9)

5. The Electric Polarizability of the Neutron:

Due to its internal structure the neutron has an extended charge distribution, which should be polarizable in an external electric field. In the Coulomb field of a heavy nucleus the interaction potential, due the the electric polarizability, is given by $V_{pot} = -\frac{1}{2}\alpha_n Z^2 e^2/r^4$. The corresponding scattering amplitude was first calculated by Thaler [17] and by Breit and Rustgi [18] and is nearly proportional to $Z^{5/3}$. For $\alpha_n = 1\times10^{-3}$ fm^3, as suggested by the electric polarizability of the proton and quark model calculations [19], it contributes about 0.5% to the scattering length and 1% to the scattering cross-section of lead. The scattering amplitude for $qR_N << 1$ (R_N being the nuclear charge radius and $\hbar q$ the momentum transfer), is given by [1,20]

$$f(q) = \alpha_n Z^2 \quad \frac{e^2 m}{\hbar^2} \frac{1}{R_N}\left[\frac{6}{5} - \frac{\pi}{4}qR_N + \frac{4}{7}(qR_N)^2 + O(qR_N)^4\right] \quad (5)$$

The total scattering cross-section σ_s can be parametrized:

$$\sigma_s(k) = \sigma_s(0) + ak + bk^2 + O(k^4)\,, \quad (6)$$

where k is the wave-vector of the incoming neutron. The parameter a depends only on the electric polarizability of the neutron. b comes mainly from the effective range of the neutron-nucleus interaction.

Having corrected for resonance, Schwinger and neutron-electron scattering an optimal fit of equation (6) to the whole set of data in the energy range from 50 eV to 20 keV yields [1,21]:

$$\sigma_s = 11.253(5) + 0.060(51)\ k - 371(27)\ k^2 \qquad Pb(7)$$

$$\sigma_s = 4.7435(16) + 0.006(22)\ k - 82(5)\ k^2 \qquad C\ (8)$$

k in fm^{-1}. In the carbon case (8) the term proportional to k is compatible with zero. This gives a good test for systematic errors and the quality of the data analysis. From the term proportional to k in (7) the electric polarizability can be evaluated to [21]:

$$\alpha_n = (1.2 \pm 1.0)\times10^{-3}\ \text{fm}^3 \quad (9)$$

The error given is mainly determined by the statistical accuracy of the present experiment. At that level of accuracy there are no systematic errors detected and a reduction of the errors of at least a factor 3 seems feasible. Such a project is in progress.

6. Conclusion:

A significant improvement in the accuracy and reliability of neutron time-of-flight experiments has been achieved by simultaneous TOF and analog measurement. Using highly efficient detectors like ^{10}B-loaded liquid scintillators accuracies of $\Delta\sigma/\sigma \leq 10^{-3}$ in total cross-section measurements are reached in TOF transmission experiments up to tens of keV neutron energy. This new kind of precision experiment may improve our knowledge of fundamental properties of the neutron, like its electric polarizability and the neutron-electron interaction.

Acknowledgements

One of us (J.S) wants to thank the HARWELL Nuclear Physics Devision, Dr M. Coates and the HELIOS linac group for the opportunity to perform the neutron transmission experiments and for the enjoyable collaboration help and hospitality during the stays at HARWELL. This work was supported by the Ausrian *Fonds zur Förderung der Wissenschaftlichen Forschung Projekt 5520.*

References:

[1] J. Schmiedmayer, *Die elektrische Polarisierbarkeit des Neutron*, PhD thesis, Tech. University Vienna (1987).

[2] Bourgeois F. et al, IEEE Trans.Nuc.Sci., NS-32 (1985) 631; Bourgeois F. et al, Nuc.Inst.Meth. A252 (1986) 590; Brand c. et al, Nuc.Inst.Meth. A252 (1986) 413.

[3] Delavallade G., Vanuxem J.P., Nuc.Inst.Meth. A252 (1986) 596.

[4] J. Schmiedmayer, M. Pernicka, M.C. Moxon, submitted to Nuc.Inst.Meth. (1988)

[5] J. Schmiedmayer, to be published.

[6] Cierjacks S., in *Neutron Sources For Basic Physics and Application*, Vol. 2 (1983) Pergamon Press

[7] C.O. Muehlhause and G.E. Thomas, Phys.Rev. 85 926, (1952); Nucleonics 11 44, (1953); L.M. Bollinger, and G.E. Thomas, Rev.Sci.Instr. 28 489, (1957); H.E. Jackson, and G.E. Thomas, Rev.Sci.Instr. 36 419, (1965); L.R. Greenwood, and N.R. Chellew; Rev.Sci.Instr. 50 466, (1979).

[8] A.H. Wapstra and K. Bos, Atom.Data Nuc.Data Tables 19, 218 (1977).

[9] M.C. Moxon, in *Neutron Data of Structural Materials for Fast Reactors* Geel 1977 (ed. by K.H.Böckhoff), Pergamon Press, p. 644.

[10] Sene M.R., Hawkes N.P., Findlay D.J.S. Nuc.Inst.Meth. A245 (1987) 591.

[11] Sene M.R. private comunication

[12] L. Koester, W. Waschkowski and A. Klüver, Physica 137B 282 (1986).

[13] S.F. Mughabghab, M. Divadeenam and N.E. Holden, *Neutron Cross-Sections* Vol.1, Academic Press, Part A (1983), Part B (1985).

[14] H.T. Heaton, et al., Nucl. Sci. Eng. 56 27 (1975).

[15] J.C. Lachkar, in *Neutron Standards and Applications*, NBS special publication 493, 93 (1977).

[16] H. Schumacher et al., Phys. Stat. Sol. 20 109 (1973).

[17] R.M. Thaler, Phys.Rev. 114 827 (1959).

[18] G. Breit and M.L. Rustgi, Phys.Rev. 114 830 (1959).

[19] Dattoli G., Matone G. and Prosperi D., Lett.Nuovo Cimento 19 601 (1977); Schäfer A. et al., Phys.Lett. 143B 323 (1984); Weiner R. and Weise W., Phys.Lett. 159B 85 (1985); M. Damashek and F.J. Gilman, Phys.Rev. D1 1319 (1970); J. Bernabeu and T.E.O. Ericson, Phys.Lett. 42, 93 (1972); U.E. Schröder, Nucl.Phys. B166 103 (1980).

[20] H. Leeb, G. Eder and H. Rauch, J. de Physique 45 C3-47 (1984).

[21] J. Schmiedmayer, H. Rauch, P. Riehs, submitted to Phys. Rev. Lett. (1988)